The remarkable X-ray spectrum of the Broad-Line Radio Galaxy 3C 445

R. M. Sambruna, J. N. Reeves, V. Braito

NASA/GSFC, Code 661, Greenbelt, MD 20771 (rms@milkyway.gsfc.nasa.gov)

Received _____; *accepted* _____

ABSTRACT

The nearby (z=0.057) radio-loud source 3C 445, optically classified as a Broad-Line Radio Galaxy, exhibits an X-ray spectrum strongly reminiscent of an obscured AGN, suggesting we are seeing this source at a relatively large angle from the radio jet. Here we present an archival 15 ks *XMM-Newton* observation of 3C 445 which confirms the remarkable complexity of its X-ray emission. The X-ray emission is described by a power law continuum with $\Gamma \sim 1.4$, absorbed by several layers of cold gas, plus strong cold reflection. A narrow, unresolved Fe Kα emission line is detected, confirming previous findings, with EW $\sim$ 400 eV. A soft excess is present below 2 keV over the extrapolation of the hard X-ray power law, which we model with a power law with the same photon index and absorbed by a column density $N_H5 \sim 10^{20}$ cm^{-2} in excess to Galactic. Remarkably, a host of emission lines are present below 2 keV, confirming previous indications from *ASCA*, due to H- and He-like O, Mg, and Si. The detection of two features at 0.74 and 0.87 keV, identified with OVII and OVIII Radiative Recombination Continuum features, suggest an origin of the lines from a photoionized gas, with properties very similar to radio-quiet obscured AGN. Two different ionized media, or a single stratified medium, are required to fit the soft X-ray data satisfactorily. The similarity of the X-ray spectrum of 3C 445 to Seyferts underscores that the central engines of radio-loud and radio-quiet AGN similarly host both cold and warm gas.

*Subject Headings:*Galaxies: active — galaxies: radio – galaxies: individual — X-rays: galaxies

1. Introduction

The X-ray emission from AGN is a powerful tool to investigate the structure and physical conditions of the matter in the proximity of the central supermassive black hole. In particular, sensitive X-ray spectroscopy has been very successful in disentangling the contributions from warm and cold matter in Seyferts. At soft X-rays, more than 50% of these sources exhibit complex intrinsic absorption/emission features suggesting the presence of a photoionized gas (Crenshaw et al. 2003), containing a significant fraction of the accretion mass. In a handful of sources, blueshifted absorption features were observed, indicating an outflow from the nucleus with quasi-relativistic velocities, $v/c \gtrsim 0.1$ (Chartas et al. 2002, Pounds et al. 2003, Reeves, O'Brien, & Ward 2003; see also Braito et al. 2007 and references therein). The same absorbing gas is thought to be responsible for the soft X-ray emission lines observed in type-2 sources (Guainazzi et al. 2005; Turner et al. 1997), via scattering or reflection (Netzer 1996). Reflection features at hard X-rays (Fe Kα line, Compton hump) indicate reprocessing by cold gas in an accretion disk (George & Fabian 1991, Nandra et al. 1997), and provide a way to explore the innermost regions around the black hole where gravitational effects are most important. A prominent, broad Fe Kα emission line at 6.4 keV, together with a hump peaking around 20–30 keV (the "Compton hump") indicate reprocessing of the optical-UV emission in colder gas arranged in an accretion disk. A pc-scale molecular torus encases the accretion flow, spurring orientation-based unification models.

In contrast, the inner regions of radio-loud AGN are much more poorly studied, because of the relative rarity and distance of these sources. Broad-Line Radio Galaxies (BLRGs) are by now thought to exhibit weaker reflection features and flatter X-ray continua than Seyfert 1s (e.g., Sambruna, Eracleous, & Mushotzky 2002, and references therein). No evidence for warm absorbers was detected so far in bright BLRGs at energies $\lesssim 2$ keV with *ROSAT* and

ASCA (Sambruna et al. 1999, S99 in the following; Reynolds 1997), *BeppoSAX* (Grandi, Malaguti, & Fiocchi 2006), and with *Chandra* and *XMM-Newton* (Gliozzi et al. 2007; Lewis et al. 2005; Ogle et al. 2005; Ballantyne et al. 2004). A recent 120 ks *Suzaku* observation of 3C 120 shows a featureless continuum at soft X-rays, attributed to the radio jet (Kataoka et al. 2007). It may thus seem that, contrary to Seyferts, the central engines of BLRGs are devoid of (warm) gas.

However, there are reasons to expect the presence of a medium in BLRGs and other radio-loud AGN. For example, centrifugally-driven winds, lifting matter off the disk's surface and channeling it down the magnetic field, are a proposed scenario for the origin of relativistic jets (Blandford & Payne 1982); at favorable orientations, these winds would lead to observable discrete absorption/emission features at soft X-rays (Königl & Kartje 1994). A dense environment can also be responsible for slowing down the inner jet via mass entrainment inferred in more beamed sources (Georganopoulos & Kazanas 2003). Unification models for radio-loud sources also postulate the presence of a warm, scattering gas to explain type-2 sources (Urry & Padovani 1995).

The lack of spectral signatures at X-rays for intrinsic warm gas in BLRGs is puzzling. A possible explanation is that X-ray spectral features from a warm circumnuclear gas are weak in radio-loud AGN, and thus difficult to detect at lower sensitivites and/or with limited bandpasses. In addition, the brightest BLRGs either lie at low Galactic latitudes and/or have strong and variable soft excess, possibly jet-related (Kataoka et al. 2007; Gliozzi et al. 2007).

The study of the gas environs of BLRGs would benefit from X-ray observations of a source seen at optimal angles, such allow us to peek into the central engine while at the same time minimizing the jet contribution in the soft X-ray band. This opportunity is offered by 3C 445, a nearby (z=0.057) and X-ray bright BLRG, $F_{2-10\ keV} \sim 7 \times 10^{-12}$ erg

cm^{-2} s^{-1}. Optical and radio studies, as well as its *ASCA* spectrum, suggest this source is seen almost edge-on, with the line of sight grazing the outer edge of the torus. Using an archival *XMM-Newton* 15 ks spectrum, we discovered a host of soft X-ray emission lines from 3C 445 which suggest the presence of ionized gas around the nucleus.

Here we present and discuss the *XMM-Newton* data. The paper is structured as follows. The sources properties and the observations are summarized in §§ 2 and 3. The results of the spectral fits are presented in § 4, while discussion and conclusions follow in §§ 5 and 6. Throughout this paper, a concordance cosmology with $H_0 = 71$ km s^{-1} Mpc^{-1}, Ω_Λ=0.73, and Ω_m=0.27 (Spergel et al. 2003) is adopted. The energy spectral index, α, is defined such that $F_\nu \propto \nu^{-\alpha}$.

2. 3C 445

The nearby (z=0.057) radio galaxy 3C 445 has an FRII radio morphology (Kronberg, Wielebinski, & Graham 1986), with a linear extension up to 10′. With a steep radio spectrum between 2.7 and 4.8 GHz (α_r=0.7) and a core-to-lobe intensity ratio R=0.039 (Morganti, Killeen, & Tadhunter 1993), the source is clearly lobe dominated; from the ratio of lobe/counterlobe an inclination $i > 60°$ is inferred for the jet (Eracleous & Halpern 1998).

Broad emission lines were observed in the optical unpolarized flux (Eracleous & Halpern 1994; Corbett al. 1998), leading to its classification as a BLRG. The spectrum is very red, and steepens dramatically at UV energies (Crenshaw, Peteron, & Wagner 1988). It has been suggested that the large IR emission is the result of the reprocessing of the optical and UV emission by circumnuclear dust (Elvis et al. 1984). The optical continuum is polarized (Brindle et al. 1990). The amount of reddening derived from the large Balmer decrement ($H\alpha/H\beta \sim 8$; Crenshaw et al. 1988, Osterbrock, Koski, & Phillips 1976) and by

the large Paα/Hβ ratio (5.6; Rudy & Tokunaga 1982) is E(B-V)=1 mag. For a standard dust-to-gas conversion ratio a column density $N_H \sim 5 \times 10^{21}$ cm^{-2} is derived. This is one order of magnitude larger than the Galactic column density in the direction to the source, $N_H^{Gal} = 5.33 \times 10^{20}$ cm^{-2}, derived from 21 cm measurements (Murphy et al. 1996). Based on these properties, and on the limit to the viewing angle, we suggest we are seeing 3C 445 almost edge-on. Thus, the beamed jet is not expected to contribute significantly to the emission from the source.

At odds with its classification as a type-1 source, 3C 445 exhibits an X-ray spectrum very similar to Seyfert 2s. Previous *ROSAT* and *ASCA* observations (Sambruna et al. 1998, S98 in the following), while of insufficient quality to allow a full spectral decomposition, indicated a heavily absorbed ($N_H \sim 10^{23}$ cm^{-2}) continuum above 3 keV, plus a narrow Fe Kα line with EW $\sim$ 250 eV, and a soft excess modeled with an unabsorbed power law. From a later reanalysis of the data, S99 noted weak emission lines below 2 keV in the non-simultaneous *ROSAT* and *ASCA* data, attributed to ionized elements from O to Si. The limited quality of the data, however, prevented a detailed analysis of the lines and their origin.

Moreover, 3C 445 was detected with the Burst Alert Telescope onboard *Swift* in the energy range 15–150 keV (Tueller et al. 2007, in prep.) and with the PDS onboard *BeppoSAX* (Grandi, Malaguti, & Fiocchi 2006; Dadina 2007). However, 3C 445 lies close (30′) to the cluster of galaxies A2440 (z=0.094), and contamination of the hard X-ray flux by the cluster can not be ruled out in the *BeppoSAX* data. Nevertheless, the broad-band *BeppoSAX* spectrum was fitted with a partial-covering, dual-absorber model, yielding $\Gamma = 1.7$ and $N_H \sim 10^{23}$ cm^{-2}. These data also gave the first measure of the reflection continuum (after subtraction of the expected cluster contribution); the latter is weakly constrained, with $R \sim 3$ and large uncertainties.

Thus, previous X-ray observations of 3C 445 provided tantalizing clues that the 0.5–10 keV emission from this BLRG is complex. Moreover, analysis of the *XMM-Newton* field of view of 3C 445 reveals the presence of a nearby (1.3′) soft X-ray AGN (Grandi et al. 2004), which was not resolved at the *ASCA* and *BeppoSAX* poor angular resolutions. Thus, the *XMM-Newton* observation presented here yields the very first high-quality X-ray spectrum of this source.

3. Observations

XMM-Newton observed 3C 445 on December 6, 2001 for a total exposure of 23.8 ks. After screening the data, the net exposure which includes correction for deadtimes was 15.3 ks with the EPIC pn, 21.3 ks with MOS1, and 21.2 ks with MOS2. The count rate of the source in 0.3–10 keV is 0.626 ± 0.006 c/s with the pn and 0.18 ± 0.003 c/s with both MOS CCDs. As not enough counts were collected with the RGS (< 200) for a detailed analysis, here we concentrate on the EPIC data only.

The pn, MOS1 and MOS2 cameras were operating in Small Window mode, with the Thin filter applied. The *XMM-Newton* data have been processed and cleaned using the latest Science Analysis Software (SAS ver 7.0) and analyzed using standard software packages (FTOOLS ver. 6.1, XSPEC ver. 11.3). In order to define the threshold to filter for high-background time intervals we extracted the 10–12 keV light curve and filtered out the data when the light curve is 2σ above its mean. The inspection of this light curve shows that there was no flaring activity during this observation. For the scientific analysis only events corresponding to pattern 0–12 for the EPIC MOS and pattern 0–4 for the pn were used. EPIC pn source spectra were extracted using a circular region of 30″, background data were extracted from a circular region with radius 1′ centered at $\sim 2.5'$ from the source. This is sufficient to include most of the PSF, while excluding the 1.3′ X-ray source 1WGA

J2223.7-0206 (Grandi et al. 2004). The EPIC MOS1 and MOS2 data were extracted using a source extraction region of 30″ radius and two background regions with identical size (30″), selected on the nearby CCDs. Response matrices and ancillary response files at the source position have been created using the sas tasks `arfgen` and `rmfgen`.

The EPIC MOS1 and MOS2 data were then combined and the background subtracted spectrum binned to have at least 20 counts in each energy bin, while the background subtracted EPIC pn data were binned to have at least 30 counts per bin. Finally, we checked that there were no discrepancies between spectra extracted with this selection and spectra extracted with pattern 0.

4. Spectral Fitting Results

We first fitted the EPIC pn and MOS spectra with a simple power law plus Galactic absorption. As expected, this was not a good fit, yielding $\Gamma = -0.24$ and $\chi^2_r = 3.9/564$. Figure 1 shows the data, with the model removed for clarity. At energies above 3 keV, a curved continuum is visible indicating heavy absorption. The Fe line around 6 keV is also apparent. At soft X-rays, several emission features can be seen in the energy range 0.6–2 keV, attributed to lighter elements from O to Si.

4.1. The Continuum

We first concentrated on modeling the continuum. At the harder energies, $\gtrsim$ 3 keV, the bumpy shape of the continuum (Fig. 1) suggests heavy absorption, as in the previous *ASCA* observations (S98). F3itting the EPIC data in 3–10 keV with a single power law plus free column density indeed yields significant absorption, $N^1_H = 1.3 \pm 1.2 \times 10^{23}$ cm^{-2}, with a photon index $\Gamma = 1.26 \pm 0.11$, χ^2_r=1.1/511. The residuals of this model clearly show

an emission line feature at 6 keV (Fig. 1), identified with the Fe Kα line detected with *ASCA* (S98). Ignoring the energy range 5–7 keV, where possible contributions from a broad relativistic Fe Kα line are often seen in Seyferts, yields an acceptable fit ($\chi^2_r = 1.0/230$) but still an unusually hard continuum, $\Gamma_h = 1.0 \pm 0.18$. Thus, the flat continuum slope above 3 keV is not an artifact of a complex profile of the Fe Kα line.

Addition of the lower energy bins shows that the 0.5–3 keV flux lies 2–3 orders of magnitude above the extrapolation of the absorbed power law, indicating the presence of a soft continuum component. This confirms the previous findings from *ASCA* and *ROSAT* joint fits, which required the presence of a steeper power law at the softer energies possibly related to scattering of the nuclear radiation by ambient gas/dust (S98). We thus added a second power law component to the fit, absorbed by a column N^2_H and with photon index tied to the index of the hard power law, $\Gamma_s = \Gamma_h$. This fit yields $\chi^2_r = 1.5/733$, still poor primarily because of unaccounted emission lines. The photon index is now $\Gamma_s = \Gamma_h = 1.31 \pm 0.05$, with an absorption column density $N^2_H \sim 5 \times 10^{20}$ cm^{-2} above the Galactic value. Leaving the soft and hard indices free to vary yields $\Gamma_s = 1.55 \pm 0.10$ and $\Gamma_h = 1.08 \pm 0.08$, both still quite flat.

The presence of the Fe Kα emission line (see below) and the PDS detection suggest that addition of a reflection continuum might be necessary. We thus added cold reflection modeled with `pexrav` (Magdziarz & Zdziarski 1995), where the abundances were fixed to solar values and the inclination angle cosθ to 0.7. The free parameters of the fit were the reflection fraction, $R = \Omega/2\pi$, and the normalization. The fit is greatly improved, $\Delta\chi^2$=205, and yields very strong reflection, $R \sim 3$. While not physical, taken at face value this would indicate a strong reflection component dominating the emission at energies $\gtrsim 8$ keV.

However, if we add a third layer of absorption to the model, specifically, a third power law with tied photon index and column density N^3_H, the strength of the reflection component

decreases, $R \sim 2$ and $N_H^3 \sim 4 \times 10^{22}$ cm^{-2}. Due to the limited bandpass of EPIC and the complexity of the spectrum there is no simple way based on the data to decide whether the 2–10 keV continuum is dominated by the reflection component, or if instead multiple layers of absorption are present. Here we adopt the latter model, specifically, three distinct cold absorbers and reflection (Table 1); as we discuss later, there is no evidence for this source to be Compton-thick and thus dominated by reflection in 2–10 keV. To discriminate among the various possibilities, which clearly have different physical implications, and measure the intrinsic AGN flux, broad-band *Suzaku* observations of 3C 445 are needed.

The best spectral decomposition of the 0.4–10 keV continuum is obtained with a model including: three powerlaws, all with the same photon index, $\Gamma \sim 1.4$, and various layers of cold absorption, $N_H = 10^{21} - 10^{23}$ cm^{-2}; strong ($R = 2$) cold reflection, which becomes dominant above 8 keV. Figure 2 shows the data fitted with the above model (and with the inclusion of the emission lines, see below), and the best-fit model itself. The best-fit parameters and their 90% uncertainty are reported in Table 1, where the observed fluxes at soft and hard X-rays are also given. We estimate the covering fractions of the three cold absorbers to be: 82% (N_H^1), 4% (N_H^2), and 14% (N_H^3).

To exclude that the line-like residuals at soft X-rays are due to an inappropriate continuum modeling, we attempted fitting the EPIC spectrum with the baseline continuum model but using an ionized reflector (`reflion`) instead of the cold one. This model is known for producing relatively strong soft X-ray emission lines for intermediate ionization states (Ross, Fabian, & Young 1999). The fit with this model is worse by $\Delta\chi^2$=30. Basically, the model fails to account simultaneously for the various ionization properties at soft and hard X-rays. Specifically, accounting for the Mg and Si lines would require a strong high-ionization Fe line at 6.7–6.9 keV, which is not observed.

Note that the measured continuum photon index is rather hard, $\Gamma \sim 1.4$, flatter

than usually observed in Seyferts or other BLRGs. From a *Suzaku* observation of 3C 120, Kataoka et al. (2007) derive $\Gamma \sim 1.7$, similar to what was obtained from *ASCA* observations of BLRGs (S99). The limited EPIC bandpass, together with the presence of complex absorption, most likely conjures to produce an apparently hard continuum. Fixing Γ to 1.7, in fact, yields an equivalent fit, with an increase of the column densities of 20%. This reflects the well-known spectral degeneracy between slope and absorption column over a limited bandpass (< 10 keV).

The total observed fluxes are $F_{0.2-2\ keV} \sim 2 \times 10^{-13}$ and $F_{2-10\ keV} \sim 7 \times 10^{-12}$ erg cm^{-2} s^{-1}. These are clearly lower limits to the true AGN fluxes in these energy bands, and fully consistent with the fluxes measured with *ASCA* and *ROSAT* (S98). A 2–10 keV observed flux lower by a factor 2 was measured in earlier *BeppoSAX* observations[1] (Grandi et al. 2006). Thus, there is evidence that the medium-hard X-ray flux varied significantly over the timescale of almost 2 years between the *BeppoSAX* and *XMM-Newton* observing epochs.

Extrapolating the best-fit model at harder X-ray energies, we find a 15–100 keV observed flux of $F_{15-100\ keV} \sim 5 \times 10^{-11}$ erg cm^{-2} s^{-1}. This is a factor 2 larger than the BAT detection threshold.

4.2. The Fe line region

In Figure 3a we plot the residuals of the baseline best-fit continuum model discussed above (a power law with three absorbers plus cold reflection), zooming in the Fe Kα

[1]Note, however, that the *BeppoSAX* and *ASCA* datasets contained a (presumably small) contribution from the 1.3′nearby source; thus, the factor 2 variations between the *BeppoSAX* and *XMM-Newton* epochs is clearly a lower limit.

emission line region. These residuals were obtained by fitting the full-band EPIC data minus the 5–7 keV region.

The prominent emission line is the Fe Kα emission line at 6.4 keV visible in both the pn and MOS data (Fig. 3). Adding a Gaussian improves the fit significantly, $\Delta\chi^2$=57 for 3 additional parameters. The line is narrow, $\sigma = 71 \pm 48$ eV, and unresolved at $> 95\%$ confidence; its observed Equivalent Width against the total continuum is EW $\sim$ 380 eV (Table 2). Adding a broad Gaussian to the narrow line does not improve the fit and its width is completely unconstrained. Figure 3b shows the residuals of this model.

In both Figure 3a-b, an absorption feature is present around 6.8 keV. The dip was modeled with an inverted Gaussian, leading to a modest ($\Delta\chi^2$=10) improvement of the fit, significant at $\sim 97\%$ confidence from the F-test. The fitted energy and EW are E=6.87 $\pm$ 0.09 keV and EW=40^{+22}_{-25} eV. If the absorption feature is true, the closest candidate for its identification would be the 1$\rightarrow$2 transition of FeXXV at 6.701 keV, blueshifted by a modest amount, $v \sim 0.02c$.

We conclude that there is tentative (2σ) evidence for an absorption dip at an observed energy 6.8 keV. However, the feature significance is hindered by the choice of the underlying continuum model; a stronger reflection component would naturally account for the dip. Broad-band, sensitive observations are needed to confirm the absorption feature.

4.3. Soft X-ray Emission Lines

At softer energies, several emission lines are present in 0.5–1 keV and further around 2 keV (Figure 1). We interpret these features as emission lines due to the lighter elements from O to Si. Table 2 lists the observed line energies, fluxes, EWs, and their identifications.

The lack of a strong FeL complex at 0.9–1 keV provides evidence against an origin

of the X-ray lines in collisionally ionized gas, such as the galaxy ISM. Adding a thermal model (apec) to the best-fit model yields χ^2_r=1.14/724, and leaves line-like residuals at 0.7 and 0.8 keV, and at 1.3 and 1.8 keV. The fitted temperature is $kT \sim 0.12$ keV, with abundances ~ 0.8 solar. Previous *ROSAT* PSPC data showed the source is consistent with being point-like (S98), although higher-resolution *Chandra* data are needed to confirm this result.

A strong possibility is an ionized medium, most likely photoionized by the intense nuclear light, as commonly observed in Seyfert galaxies. Indeed, we detect two emission features at 0.74 and 0.87 keV which we interpret as the Radiative Recombination Continuum (RRC) of OVII and OVIII, respectively (Table 2). The RRC features link unequivocally the origin of the emission lines to a plasma photoionized by the AGN, generally at a temperature of a few eV (Liedahl & Paerels 1996). At the EPIC resolution the RRC features are unresolved. In the case of OVII RRC, contribution to the flux from the nearby ($\Delta\lambda = 0.299$ Å) FeXVII 3s-2p line can not be excluded; usually, however, the OVII RRC is much brighter (factor 2 or more) than FeXVII (Guainazzi & Bianchi 2006).

We thus added a photoionization model component to describe the soft X-rays, using the code XSTAR (Bautista & Kallman 2001). The latter describes the emission lines expected from a medium whose physical conditions are summarized in the ionization parameter $\xi = L_{ph}/nR^2$ ergs cm/s, where L_{ph} is the luminosity of the photoionizing continuum, n the gas density and R its distance from the nucleus. Other parameters are the element abundances relative to solar, the column density of the gas, N_H^W, and the normalization. Since the model is clearly underconstrained by the data, we fixed the elemental abundances to their best-fit values (consistent with solar within the uncertainties), and the column density to $N_H^W = 10^{21}$ cm^{-2}, similar to the columns observed in Seyfert 1s (Reynolds 1997). Only the ionization parameter and the normalization were left free to vary.

We find that the EPIC data require two separate media, one with ionization parameter $\log \xi_1$=1.9, accounting for most of the O and Ne lines, and a second one with $\log \xi_2$=–0.09, responsible for the Mg and Si lines. The addition of a second ionized medium is significant at $> 99.9\%$ confidence. The parameters of the best-fit model with XSTAR are reported in Table 1, and the model is shown in Figure 2. The individual lines fluxes and EWs are listed in Table 2.

In conclusion, an archival 15 ks EPIC observation of 3C 445 provides evidence for a very complex X-ray spectrum. In particular, several X-ray emission lines are present in 0.5–2 keV, most likely due to a photoionized gas. To our knowledge, this is the first time that soft X-ray emission lines are detected in a radio-loud AGN. The presence of X-ray lines from 3C 445 was previously claimed based on non-simultaneous *ROSAT* and *ASCA* spectra (S99), which also indicated a heavily absorbed continuum. In addition to confirming these features, the EPIC data also provide evidence for a strong reflection continuum and/or several layers of cold absorption.

5. Discussion

Overall, the 0.5–10 keV spectrum of 3C 445 is remarkably similar to a Seyfert 2, at odds with its classification as type-1 AGN. The EPIC spectrum indicates a strong, albeit uncertain without hard X-ray observations, reflection component which is expected to dominate the continuum above 10 keV, and indeed 3C 445 was detected with the BAT and PDS experiments. Given the inclination angle of the radio source, it is quite possible that the Compton hump is due to reflection off a medium along the line of sight (the torus wall?). To this regard, the EW of the narrow Fe Kα emission line, EW $\sim$ 400 eV, is indeed consistent with being produced by reflection off a cold medium with columns $N_H \gtrsim 10^{23}$ cm^{-2} (Turner et al. 1997), being a factor 3 larger than required by transmission.

Alternatively, the requirement in the EPIC data of an unusually strong reflection component is alleviated by adding multiple cold absorbers to the continuum model (§ 4.1). This scenario would imply the presence of different layers of absorption, which could possibly totally obscure the primary nuclear X-ray continuum in the EPIC bandpass. To this regard, we tested the possibility that 3C 445 is Compton-thick, i.e., there is yet another, unaccounted absorber, $N_H \gtrsim 10^{24}$ cm^{-2}, using the diagnostic diagram of Bassani et al. (1999). This is a plot of the Fe Kα EW versus the thickness parameter T, defined as the ratio of the total 2–10 keV flux of the source and the intrinsic [OIII] flux (Bassani et al. 1999). In this plot, Compton-thick sources tend to occupy the region of large EW and smaller T values.

The observed [OIII] flux of 3C 445 is $F_{obs}[OIII] = 1.7 \times 10^{-13}$ erg cm^{-2} s^{-1} (Tadhunter et al. 1998). Correcting for the reddening using the observed Balmer decrement (§ 2), the intrinsic flux is $F_{obs}[OIII] = 3 \times 10^{-12}$ erg cm^{-2} s^{-1}. From the 2–10 keV flux in Table 1, the T parameter is T=2.2. This value and the Fe Kα EW $\sim$ 400 eV (Table 1) place 3C 445 in the region of AGN with absorption column densities $N_H \sim 10^{23}$ cm^{-2} in Figure 1 of Bassani et al. (1999). Thus, there is no evidence based on the presently available data that 3C 445 is Compton-thick.

Perhaps the most striking result of the EPIC data analysis is the detection of X-ray emission lines below 2 keV. Again, this is similar to what generally found in obscured radio-quiet AGN (Turner et al. 1997, Guainazzi et al. 2005), where photoionization is generally dominant but with a non-negligible contribution from resonant scattering, as shown by high-resolution X-ray spectra of a large sample of such systems (Guainazzi & Bianchi 2006). Indeed, the EPIC spectrum of 3C 445 is very similar to the Compton-thin Seyfert 2 NGC 4507, where emission lines from ionized O, Ne, Mg, and Si (as well as a strongly absorbed continuum) were detected with *XMM-Newton* with similar EWs (Matt

et al. 2004). As in the case of NGC 4507, two ionized emitters or a single emitter with a range of ionization parameters (Kinkabwhala et al. 2002) are required for 3C 445. The ionization parameters we measure for 3C 445 (Table 1) are within the range (ξ^1) or slightly lower (ξ^2) than typically found for type-2 Seyferts (e.g., Kinkhabwala et al. 2002).

We conclude that the central engine of 3C 445 hosts a warm gas with properties similar to radio-quiet obscured AGN, which is responsible for the observed soft X-ray lines, most likely through scattering. The location of this "warm mirror" remains unknown with the present data. Using *Chandra* and *HST* [OIII] images, Bianchi, Guainazzi, & Chiaberge (2006) showed that the soft X-ray emission of obscured radio-quiet AGN is extended and spatially coincident with the NLR. Unfortunately, no *Chandra* images are yet available to test this hypothesis in the case of 3C 445. Based on the fact that we can see the soft X-ray lines, we can at least locate the warm mirror further out from the cold gas affecting the continuum emission (Matt et al. 2004). It is possible that the ionized medium responsible for the soft X-ray lines resides in the BLRs, where $N_H \sim 10^{21}$ cm^{-2}. Another possibility is an outflow extending vertically above the plane of the torus, particularly intriguing given the radio-loud nature of 3C 445 and the presence of a radio jet (see below).

From the EPIC best-fit model, we calculated an upper limit to the distance R of the warm gas from the black hole, using the gas parameters from Table 1. Under the assumption the gas forms a thin shell, $\Delta R/R < 1$, and for a nuclear intrinsic (corrected for absorption) luminosity $L_{2-10\ keV} = 6 \times 10^{44}$ erg s^{-1}, and assuming the medium has a density similar to the BLRs ($n = 10^9$ cm^{-3}), we find $R = 0.03 - 0.3$ pc. At these distances the gas velocity should be $v \sim$ 4,000–12,000 km/s for a black hole mass 10^9 M$_\odot$. If instead $n = 10^3$ cm^{-3}, consistent with the NLRs, then $R > 30$ pc and $v < 500$ km/s. These scenarios can be tested with detailed X-ray spectroscopy (e.g., *Chandra* gratings), which will resolve the individual lines yielding the density and location of the photoionized gas, and will measure

intrinsic velocity dispersions/energy shifts.

The detection of soft X-ray lines in 3C 445 has implications for other BLRGs in the context of unification models. In radio-quiet Seyferts, the "warm mirror", is commonly unified with the ionized outflows producing the absorption features observed in the soft X-ray spectra of type-1 objects, the "warm absorber" (Netzer 1996; Guainazzi & Bianchi 2007). Assuming the general unification scenario of Seyferts holds for radio-loud AGN as well (Urry & Padovani 1995), and that 3C 445 is fairly representative of other radio-loud AGN, one can infer that a warm absorbing gas should be present in the more aligned counterparts of 3C 445, producing absorption features at soft X-rays. If this is indeed the case, one may wonder why these features were not detected in BLRGs. The answer is twofold. On one hand, there are only 4 bright BLRGs traditionally known: 3C 120, 3C 382, 3C 390.3, and 3C 111, all of them observed extensively at X-rays. However, a strong soft excess is present in 3C 120 (attributed to the jet; Kataoka et al. 2007) and in 3C 382 (Gliozzi et al. 2007), masking any possible contribution from a warm absorber; the superluminal radio source 3C 111 lies at low Galactic latitudes, preventing a detailed study of the emission below 2 keV. On the other hand, deep X-ray observations of BLRGs with a signal-to-noise ratio comparable to Seyfert 1s were never performed in the past, hampering the detection of weak features. High-resolution grating observations of BLRGs were so far performed only for 3C 382 (HETGS) and 3C 390.3 (RGS); a detailed study in under way.

The best candidate BLRG for the detection of absorption features is arguably 3C 390.3. In fact, this galaxy has a low ($N_H = 3.7 \times 10^{20}$ cm^{-2}) Galactic column, a relatively large X-ray flux ($F_{2-10\ keV} \sim 10^{-11}$ erg cm^{-2} s^{-1}), and a powerlaw continuum (S99). Previous X-ray observations of 3C 390.3, however, provide controversial evidence for the presence of absorption. A variable column density was observed in multiepoch X-ray spectra of this BLRG (Grandi et al. 1999), while a 40 ks *ASCA* spectrum provided evidence for an

absorption edge at 0.74 eV with optical depth $\tau \sim 0.3$, identified eith the OVII edge at 0.739 eV (S99). However, no apparent absorption but instead weak emission lines were detected at soft X-rays in a 90 ks *XMM-Newton* EPIC exposure (Lewis et al. 2007, in prep.). Our recently performed *Suzaku* observation will provide the best X-ray dataset to-date to investigate the soft X-ray spectrum of this BLRG.

We now comment on the apparent discrepancy of the X-ray spectrum with the optical type-1 classification of 3C 445. This difficulty may be circumvented in the "clumpy hydromagnetic wind" torus model of Elitzur & Shloshman (2007; see also Königl & Kartje 1994, Everett 2005). In this model, the torus is not a continuous, donut-like structure but is composed of clouds distributed around the equatorial plane of the AGN (see Fig. 3 in Elitzur 2006); the torus extends in the inner regions beyond the dust sublimation radius, where the clouds become atomic and ionized yielding broad optical lines and warm X-ray absorption. For a given number of clouds and their distribution on the equatorial plane, classification of an AGN as type 1 or 2 depends on whether the line of sight intercepts enough obscuring clouds.

The multiwavelength properties of 3C 445 can be reconciled within this scenario. The inclination angle of 3C 445 from the radio is larger, $\gtrsim 60°$ (Eracleous & Halpern 1998), than the current estimates of the average opening cone of the "torus", $\sim 30 - 45°$ (Schmitt et al. 2001), implying we might be looking at the nucleus of 3C 445 through significant number of clouds. Our line of sight could be such to be obscured by matter in the outer, colder ($N_H \sim 10^{23}$ cm^{-2}) molecular clouds of the toroidal distribution, while at the same time intercepting the broad emission lines from innermost ionized BLR clouds if the latter are lifted at some height above the plane (Elitzur & Shlosman 2007). The BLR clouds could also be responsible for the lower column density, $N_H^1 \sim 5 \times 10^{20}$ cm^{-2}, and scattering power law component derived from the EPIC data (Table 1). The external dustier clouds

would be responsible for the observed continuum and Hα polarization, as well as for the strong IR continuum emission.

The clumpy wind scenario provides an explanation also for the X-ray emission lines from 3C 445. Königl & Kartje (1994) suggested that the X-ray warm absorber/emitter observed in Seyferts coincides with clouds uplifted from the surface of the accretion disk by the magnetic field in a hydromagnetically driven sub-relativistic outflow. X-ray observations at moderate-to-high spectral resolution of Seyferts 1/2 detected signatures of winds. A large proportion of these sources exhibit soft X-ray absorption lines blueshifted relative to systemic, indicative of low-velocity, $\sim$ 1,000 km/s, outflows; at larger luminosities, fast outflows ($v \gtrsim 0.1c$) were observed in a small number of systems on the basis of FeK absorption features (see Braito et al. 2007 and references therein).

Indeed, in the clumpy wind model, the conditions for developing such an outflow become particularly favorable toward the inner parts of the disk (Elitzur & Shlosman 2007). From this perspective, it is tantalizing to speculate that the X-ray emission lines observed from 3C 445 originate from an inner outflow component, perhaps related to the formation of the radio jet itself (Blandford & Payne 1984; Königl & Kartje 1994; Proga et al. 2000). The EPIC data, however, do not provide conclusive evidence for the presence of an outflow in 3C 445. A weak absorption feature is observed at 6.8 keV, but its significance is hindered by the choice of the underlying continuum model (§ 4.2). Broad-band, higher-resolution X-ray observations will enable us to better characterize the cold and warm media in 3C 445.

6. Conclusions

Using an archival, 15 ks *XMM-Newton* spectrum we have shown that the X-ray emission from the nearby BLRG 3C 445 is quite complex. In particular, its properties

are remarkably similar to those of obscured radio-quiet AGN, with a heavily absorbed continuum and possibly a strong reflection component, a narrow Fe Kα emission line, and several soft X-ray lines consistent with reflection/scattering off a warm "mirror".

Of particular interest is the detection, for the first time in a BLRG and indeed in a radio-loud AGN, of X-ray emission lines in the 0.5–2 ke bandV, with properties very similar to radio-quiet Seyferts 2. The most likely origin of the lines is from a photoionized gas close to the nucleus. Follow-up X-ray spectroscopy of 3C 445 with higher resolution is strongly encouraged to determine the location and density of the warm medium.

If unification models hold, and if 3C 445 is representative of radio-loud AGN, one would expect to observe absorption features from the same "warm mirror" in BLRGs more favorably oriented close to the line of sight. So far, such features have eluded detection. Future *Suzaku* observations of radio-loud AGN of both type 1 and 2 will allow us to investigate the gas content of these systems.

This research has made use of data obtained from the High Energy Astrophysics Science Archive Research Center (HEASARC), provided by NASA's Goddard Space Flight Center, and of the NASA/IPAC Extragalactic Database (NED) which is operated by the Jet Propulsion Laboratory, California Institute of Technology, under contract with the National Aeronautics and Space Administration.

REFERENCES

Ballantyne, D.R., Fabian, A. C., & Iwasawa, K. 2004, MNRAS, 354, 839

Bassani, L. et al. 1999, ApJS, 121, 473

Bautista, M.A. & Kallman, T.R. 2001, ApJS, 134, 139

Bianchi, S., Guainazzi, M., & Chiaberge, M. 2006, A&A, 448, 499

Blandford, R.D. & Payne, D.G. 1982, MNRAS, 199, 883

Braito, V. et al. 2007, ApJ, submitted

Brindle, C., Hough, J. H., Bailey, J. A., Axon, D. J., Ward, M. J., Sparks, W. B., & McLean, I. S. 1990, MNRAS, 244, 577

Chartas, G., Brandt, W. N., Gallagher, S. C., & Garmire, G. P. 2002, ApJ, 579, 169

Corbett, E.A., Robinson, A., Axon, D.J., Young, S., & Hughes, J.H. 1998, MNRAS, 296, 721

Crenshaw, M. et al. 2003, ARA&A, 41, 117

Crenshaw, M., Peterson, B. M., & Wagner, R. M. 1988, AJ, 96, 1208

Dadina, M. 2007, A&A, 461, 1209

Elitzur, M. & Shlosman, I. 2007, ApJ, in press (astroph/0605686)

Elitzur, M. 2006, in The Central Engine of AGN, ASP Conference Series, eds. L.C.Ho and J.-M. Wang (astroph/0612458)

Elvis, M., Willner, S. P., Fabbiano, G., Carleton, N. P., awrence, A., & Ward, M. J. 1984, ApJ, 280, 574

Eracleous, M. & Halpern, J.P. 1998, ApJ, 505, 577

Eracleous, M. & Halpern, J. P. 1994, ApJS, 90, 1

Everett, J. 2005, ApJ, 631, 689

Georganopoulos, M. & Kazanas, D. 2003, ApJ, 594, L27

George, I. M. & Fabian, A.C. 1991, MNRAS, 249, 352

Gliozzi, M., Sambruna, R.M., Eracleous, M., & Yaqoob, T. 2007, ApJ, submitted

Grandi, P., Malaguti, G., & Fiocchi, M. 2006, ApJ, 642, 113

Grandi, P., Foschini, L., Masetti, N., & Palazzi, E. 2004, A&A 418, 907

Grandi, P. et al. 1999, A&A, 343, 33

Guainazzi, M. & Bianchi, S. 2007, MNRAS, 374, 1290

Guainazzi, M. & Bianchi, S. 2006, astroph/0612488

Guainazzi, M., Fabian, A.C., Iwasawa, K., Matt, G., & Fiore, F. 2005, MNRAS, 356, 295

Kataoka, J. et al. 2007, PASJ, in press (astroph/0612754)

Kinkhabwala, A. et al. 2002, ApJ, 575, 732

Königl, A. & Kartje, J.F. 1994, ApJ, 343, 446

Kronberg, P. P., Wielebinski, R., & Graham, D. A. 1986, A&A, 169, 63

Lewis, K.T., Eracleous, M., Gliozzi, M., Sambruna, R.M., & Mushotzky, R.F. 2005, ApJ, 622, 816

Liedahl, D.A. & Paerels, F. 1996, ApJ, 468, L33

Magdziarz, P. & Zdziarski, A. 1995, MNRAS, 273, 837

Matt, G., Bianchi, S., D'Ammando, F., & Martocchia, A. 2004, A&A, 421, 473

Morganti, R., Killeen, N. E. B., & Tadhunter, C. N. 1993, MNRAS, 263, 1023

Murphy, E. M., Lockman, F. J., Laor, A., & Elvis, M. 1996, ApJS, 105, 369

Nandra, K., George, I.M., Mushotzky, R.F., Turner, T.J., & Yaqoob, T. 1997, ApJ, 477, 602

Netzer, H. 1996, ApJ, 473, 781

Ogle, P.M. et al. 2005, ApJ, 618, 139

Osterbrock, D. E., Koski, A. T., & Phillips, M. M. 1976, ApJ, 206, 898

Pounds, K. A., Reeves, J. N., King, A. R., Page, K. L., O'Brien, P. T., & Turner, M. J. L. 2003, MNRAS, 345, 705

Proga, D., Stone, J.M., & Kallman, T.R. 2000, ApJ, 543, 686

Reeves, J. N., O'Brien, P. T., & Ward, M. J. 2003, ApJ, 593, L65

Reynolds, C. 1997, MNRAS, 286, 513

Ross, R.R., Fabian, A.C., & Young, A.J. 1999, MNRAS, 306, 461

Rudy, R. J. & Tokunaga, A. T. 1982, ApJ, 256, L1

Sambruna, R.M., Eracleous, M., & Mushotzky, R.F. 2002, NewAR, 46, 215

Sambruna, R.M., Eracleous, M., & Mushotzky, R. 1999, ApJ, 526, 60 (S99)

Sambruna, R.M., George, I.M., Mushotzky, R.F., Nandra, K., & Turner, T.J., 1998, ApJ, 495, 749 (S98)

Schmitt, H.R. et al. 2001, ApJ, 555, L163

Spergel, D. N., et al. 2003, ApJS, 148, 175

Tadhunter, C.N., Morganti, R., Robinson, A., Dickson, R., Villar-Martin, M., & Fosbury, R.A.E. 1998, MNRAS, 298, 1035

Turner, T. J., George, I.M., Nandra, K., & Mushotzky, R.F. 1997, ApJ, 488, 164

Urry, C.M. & Padovani, P. 1995, PASP, 107, 803

This manuscript was prepared with the AAS LaTeX macros v5.2.

Table 1: EPIC Best-fit Parameters†

Parameter	
N_H^1	$22.7^{+2.1}_{-1.7} \times 10^{22}$ cm^{-2}
N_H^2	$5.0 \pm 2.0 \times 10^{20}$ cm^{-2}
N_H^3	$4.0^{+2.1}_{-1.7} \times 10^{22}$ cm^{-2}
Γ	1.42 ± 0.16
R_{refl}	$2^{+3}_{-1.5}$
E_{fold}	100 keV
cos$i$	0.7 fix
E_L	6.38 ± 0.03 keV
σ_L	71 ± 48 eV
EW*	380^{+75}_{-71} eV
$\log \xi^1$	$1.94^{+0.12}_{-0.25}$ erg cm/s
$\log \xi^2$	$-0.09^{+0.21}_{-0.45}$ erg cm/s
N_H^W	1×10^{21} cm^{-2} fix
χ^2_r	1.00/548
$F_{0.3-2\ keV}$	2×10^{-13} erg cm^{-2} s^{-1}
$F_{2-10\ keV}$	6.7×10^{-12} erg cm^{-2} s^{-1}

Notes: †=The best-fit model consists of: three power laws with tied photon index absorbed by N_H^1, N_H^2, and N_H^3, plus cold reflection, plus two warm emitters modeled with the code XSTAR. All components are absorbed by Galactic $N_H^G = 5.33 \times 10^{20}$ cm^{-2}; *=The EW is calculated with respect to the total observed continuum.

Table 2: Soft X-ray emission lines

Energy (keV)	Flux (10^{-6} ph cm^{-2} s^{-1})	EW† (eV)	Identification
0.57 ± 0.03	$17.8^{+0.5}_{-0.6}$	109^{+39}_{-29}	OVII Kα
0.74 ± 0.03	3.7 ± 2.0	33^{+22}_{-8}	OVII RRC
0.87 ± 0.01	5.5 ± 1.7	62 ± 20	OVIII RRC
1.34 ± 0.03	2.5 ± 1.1	49 ± 22	Mg XI
1.78 ± 0.03	2.9 ± 1.1	83 ± 30	Si XIV
6.38 ± 0.03	13.1 ± 0.4	380^{+75}_{-71}	Fe Kα

Notes: †=The EWs are measured against the total observed continuum at their respective energies.

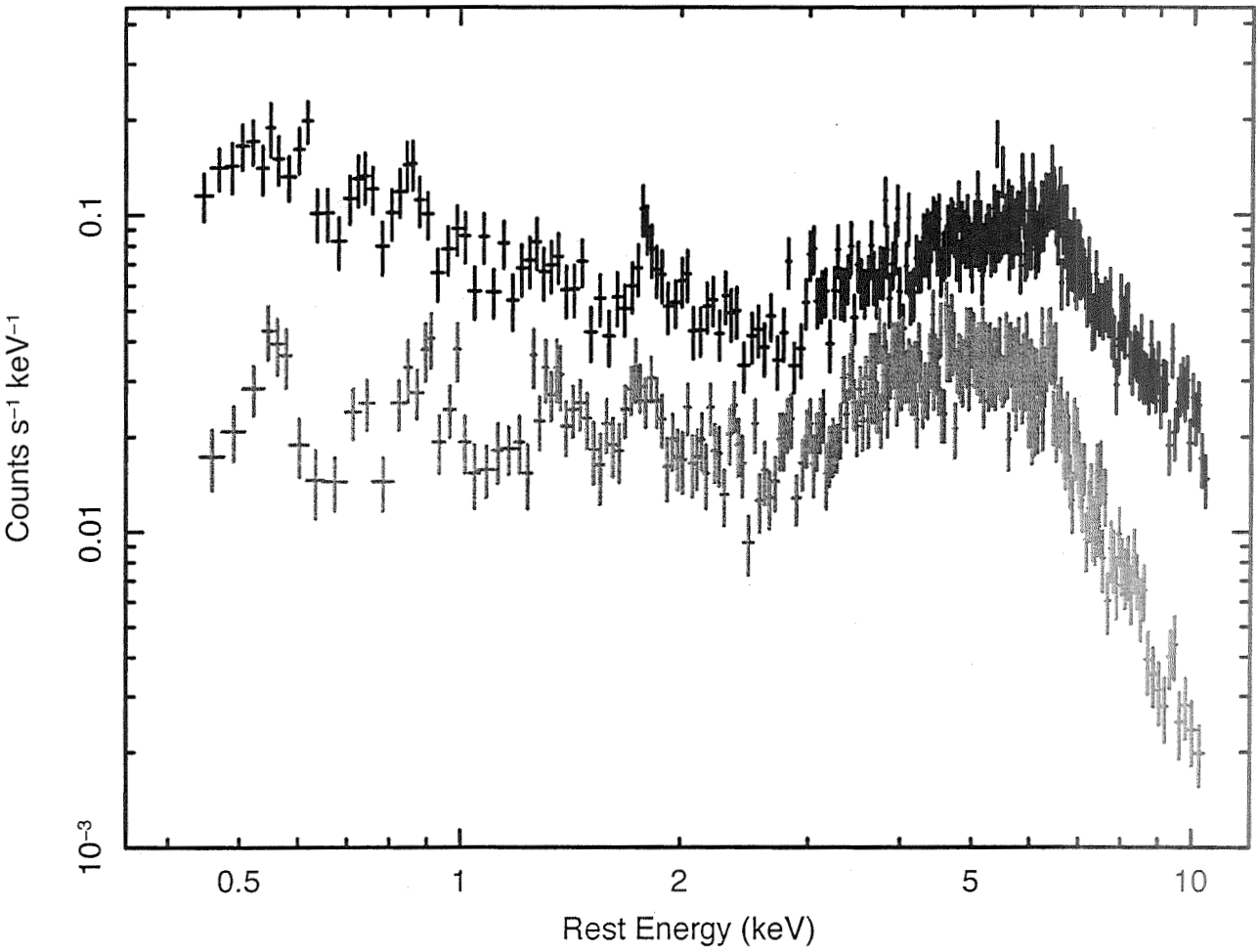

Fig. 1.— The EPIC spectra of 3C 445, from an archival 15 ks observation. The spectrum with higher flux is the pn, while the remaining spectrum are the MOS1,2. The data were fitted with the baseline model of a single power law with Galactic absorption; for clarity the model is not shown here. A complex X-ray spectrum is apparent, with a bumped continuum above 3 keV, the Fe Kα line, and several emission lines in 0.6–3 keV.

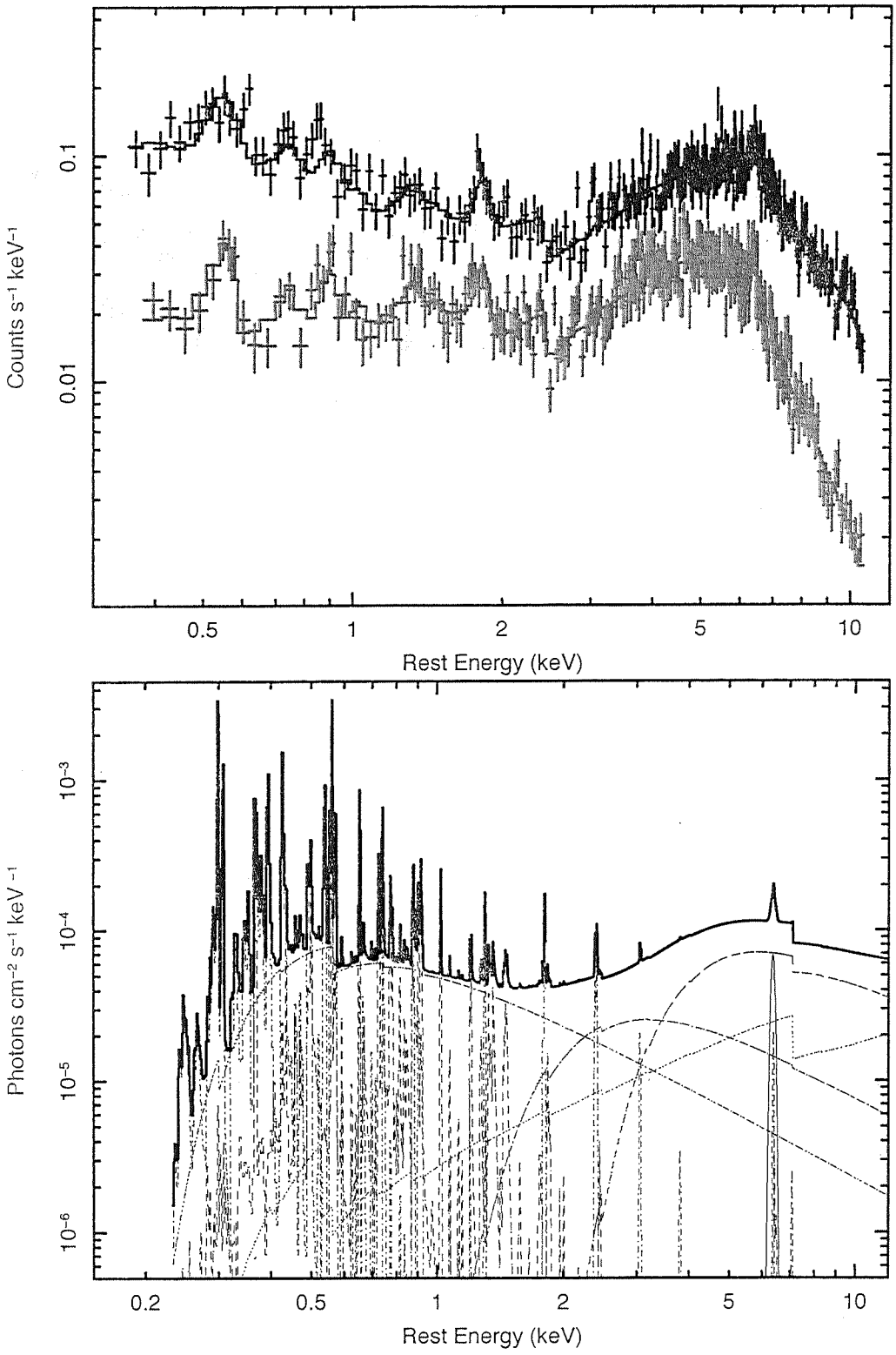

Fig. 2.— EPIC pn and MOS1+2 data (top panel) and best-fit model (bottom panel).

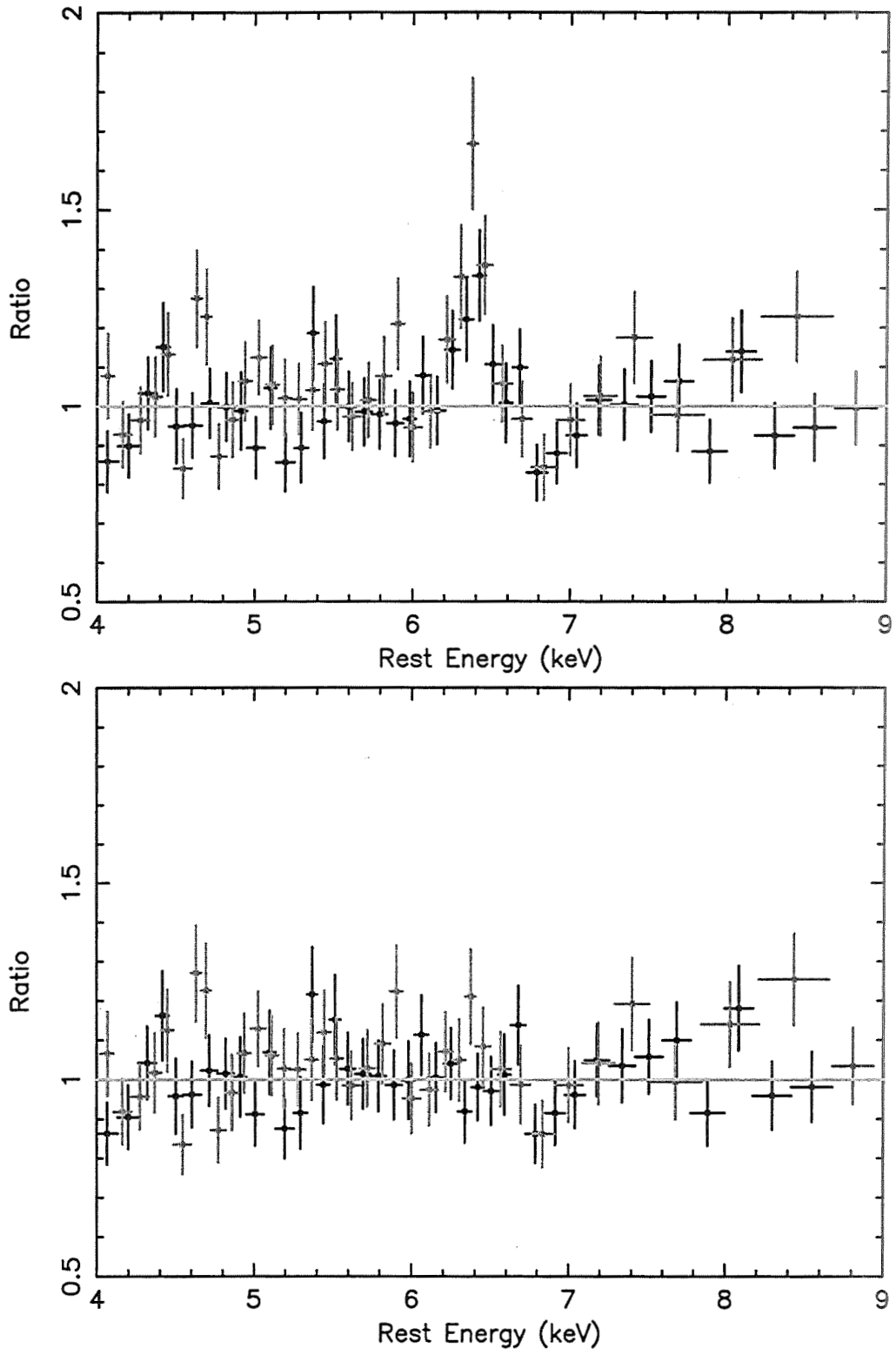

Fig. 3.— *(Top, a):* Residuals of a fit to the EPIC data of 3C 445 with the best-fit continuum model (Table 1) in the region of the Fe Kα line. A narrow line is visible, together with an absorption dip at 6.8 keV. *(Bottom, b):* Residuals of the same model, but with a narrow Gaussian line added at 6.1 keV.